Plasma Astrophysics
A. O. Benz, Kluwer Academic publishers
2002

CHAPTER 1

INTRODUCTION

People who have the chance to see the solar corona during a total solar eclipse are fascinated by its brilliant beauty. Appropriately, the word 'corona' is the Latin root of the English 'crown'. Its optical luminosity is less than a millionth of the Sun's total flux and is normally outshone by atmospheric stray light. In a total solar eclipse, on average about once every 18 months, a narrow strip of the Earth's surface is shielded completely by the Moon from the brilliant disk of the Sun, and the corona appears. The phenomenon has been known from antiquity, and is described by Philostratus and Plutarch with considerable astonishment. Almost identical prehistoric paintings in Spanish caves and on rocks in Arizona, USA, seem to represent the Sun surrounded by coronal streamers and to testify to human emotions of even older times. Nevertheless, solar eclipses are rare, and the corona escaped scientific scrutiny and even interest until the middle of the 19th century, when it became clear that it is a solar phenomenon, not related to the Moon, nor an artifact produced by the Earth's atmosphere. It entered the limelight in 1939 when W. Grotrian and B. Edlén identified coronal optical lines as originating from highly ionized atoms, suggesting a thin plasma of some million degrees. The temperature was confirmed in 1946 by the discovery of thermal radio emission at meter waves. This unexpectedly high temperature is still an enigma today: it is one of the reasons why the solar corona will be a primary target of solar research in the coming years.

Stellar flares and activity observed at optical and radio wavelengths have long been taken as hints for the existence of solar-like coronae of other stars. The recent advent of X-ray and UV observing satellites, and the advancement of optical spectroscopy and radio interferometers, have finally made it possible to detect and study the quiescent emissions of stellar coronae and transition regions. They have shown persuasively that main sequence stars with less mass than about 1.5 times the mass of the Sun (astronomically speaking 'later' than about spectral type F5, and beyond type M) probably all have coronae. The extremely hot and massive coronae of young, rapidly rotating stars are of particular interest.

1.1. The Solar Corona

1.1.1. Brief overview of the Sun

The Sun is a gaseous body of plasma structured in several, approximately concentric layers. In the central *core*, hydrogen nuclei are fused into helium nuclei, providing the energy for the solar luminosity and for most of the activity in the outer layers. The size of the core is about a quarter of the radius of the visible disk, $R_\odot$. From there, the energy is slowly transported outward by radiative diffusion. Photons propagate, are absorbed and remitted. The *radiation zone* extends to 0.71 $R_\odot$, as revealed by the seismology of surface oscillations. The temperature decreases from $1.55 \cdot 10^7$ K in the center to some $2 \cdot 10^6$ K. At this point, the decrease becomes too steep for the plasma to remain in static equilibrium, and convective motion sets in, becoming the dominant mode of energy transport. The *convection zone* is the region where the magnetic field is generated by the combination of convection and solar rotation, called a *dynamo* process.

The solar atmosphere is traditionally divided into five layers. The reader should not imagine these as spherical shells, but as physical regimes with different characteristics. The boundaries follow the spatial structures and are extremely ragged. Figure 1.9 shows the schematic changes of density and temperature with height. Note that in reality the product of density and temperature, i.e. the pressure, does not decrease smoothly. In the outer layers, the local pressure of the magnetic field and dynamic phenomena dominate and control the pressure.

The lowest atmospheric layer, called the *photosphere*, emits most of the energy released in the core. It is the region where the solar plasma becomes transparent to optical light. The thickness of the photosphere is little more than one hundred kilometers and so forms an apparent 'optical surface'. It is just above the convection zone. Convective overshoots are observed in the photosphere as a constant, bubbling *granulation*, a coarse cell structure with a mean size of 1300 km. At larger size, supergranules suggest convective structure of a superior order. In spite of its thinness, the photosphere has been the major source of information on the Sun. The analysis of global oscillations in photospheric lines has revealed the structure of the interior. The magnetic field can be accurately measured and mapped by observing the Zeeman effect. The photosphere comprises the footpoints of the field lines extending into the regions above. Sunspots are observed as groups of dark dots having a large magnetic flux.

After reaching a minimum value of about 4300 K, the temperature surprisingly rises again as one moves up from the solar surface. The region of the slow temperature rise is called *chromosphere* after the Greek word for 'colour'. Its light includes strong lines which produce colourful effects just before and after totality of an eclipse. There are more than 3500 known lines, mostly in the optical and ultraviolet (UV) range. Of particular relevance is the Balmer-alpha line of hydrogen (Hα) at 6563 Å, which is sensitive, for example, to temperature, to plasma motion, and to impacts of energetic particles from the corona. The chromospheric

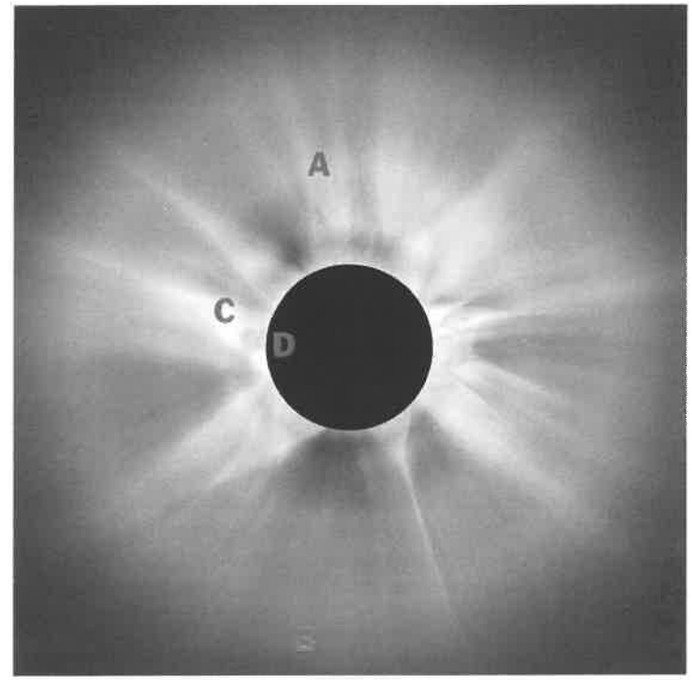

Fig. 1.1. White-light photograph of the corona taken during the eclipse of 1980, February 16 (courtesy Dr. J. Dürst). The moon blocks the bright photosphere and most of the chromosphere. Streamers (A), coronal holes (B), coronal loops (C), and prominences (D) become visible.

plasma sometimes penetrates into the upper atmosphere in the form of arch-shaped prominences (visible as bright dots at the limb of the Moon in Fig. 1.1).

Within a narrow *transition region* of only a few hundred kilometers, the temperature rises dramatically from 20 000 K at the top of the chromosphere to a few million degrees in the corona. It is the region where many emission lines in the extreme ultraviolet (EUV) originate, as the temperature is *already* high, but the density is *still* high. Most important are the Lyman-alpha line of hydrogen at 1215.7 Å and the lines of partially ionized heavier elements (e.g. O IV and C III). Another source of information is thermal bremsstrahlung emitted by free electrons as a continuum in microwaves (radio waves having frequencies in the range 1–30 GHz, introduced in Section 1.1.4). The transition region is far from being a static horizontal layer, but rather a thin envelope around relatively cool chromospheric material protruding (such as prominences) or shooting out into the corona (as observed in spicules and surges).

1.1.2. Optical observations of the corona

The solar *corona* can be observed at many wavelengths including soft X-rays, atomic lines, optical, and radio waves. Figure 1.1 shows an image in the integrated optical range (called *white light*) during an eclipse. A radial filter was used to correct for the orders of magnitude decrease in brightness with radius. The white light is produced by Thomson scattered photospheric photons on free electrons in the coronal plasma. (Another cause of white light, particularly at large angular distance, is scattering by interplanetary dust particles. It will not be discussed here.) High density structures therefore appear bright. They outline myriads of loop structures in the inner corona up to half a photospheric radius in height (1.5 $R_\odot$ from the center of the Sun). The density enhancement is a factor of 3 to 10 and outlines the magnetic field (Section 3.1.3.C). At higher altitude the high density structures consist of roughly radial streamers extending beyond 10 $R_\odot$. At their base, they blend into loop structures and resemble the helmets of old Prussian soldiers. Beyond about 1.5 $R_\odot$ the remaining magnetic field lines do not return within the heliosphere. Here the plasma is not bound and flows outwards, forming the *solar wind*. When followed back to the inner corona, one notes that most of the solar wind originates from coronal holes, regions of low density, nearly vertical magnetic fields, and conspicuous darkness in soft X-ray pictures (see Fig. 1.2). This outermost layer extends far beyond the Earth's orbit, gradually changing into the interplanetary medium, until it meets the interstellar medium at the heliopause located at some 100 to 200 astronomical units (AU).

1.1.3. Soft X-rays and EUV lines

Most of the thermal energy directly radiated by the coronal plasma is in the form of soft X-rays (photons having energies from 0.1 to 10 keV) and EUV line emission. As the contribution from the lower atmosphere is negligible, the coronal X-ray emission shown in Figure 1.2 appears on a dark background. The emission includes both a continuum emitted by free electrons and lines from highly ionized ions. The bright structures outline magnetic loops of high density (typically 10^9 electrons cm^{-3}) and high temperature ($2-3\cdot10^6$ K). Their ends are rooted in the photosphere and below.

Loops appear in different intensities and various sizes. The brightest species arch above sunspot groups and constitute the third dimension of so-called *active regions*. Whereas sunspots are cooler than the ambient photosphere, since the magnetic field inhibits convection, the active regions above sunspots – or at least some loops – are heated much more than the quiet regions of the corona. This fact strongly suggests that the heating process involves the magnetic field.

Interconnecting loops join different active regions, sometimes more than a photospheric radius apart. Systems of interconnecting loops may exist for several rotations, although individual loops often last less than one day. *Quiet region* loops are not rooted in active regions, but in magnetic elements of the quiet photosphere.

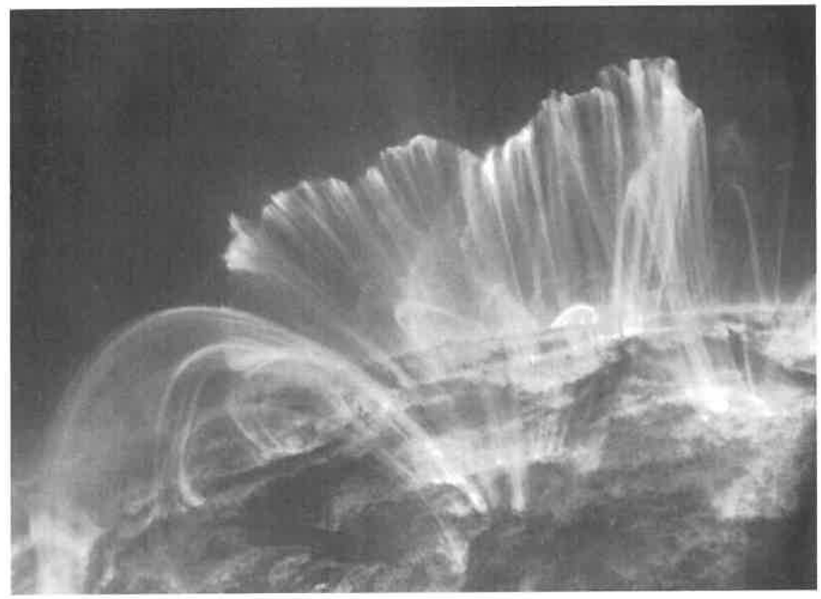

Fig. 1.2. Picture of the solar corona in the Fe IX line at 171 A taken with the TRACE satellite. The horizontal size of the frame is 0.37 $R_\odot$ ($2.6\cdot10^{10}$ cm). The solar limb is visible in the middle of the image. High density, hot loops are seen to outline the magnetic field of the corona.

Such loops are somewhat cooler ($1.5-2.1\cdot10^6$ K) and less dense. They are visible in projection above the limb as a forest of overlapping structures (Fig. 1.2).

1.1.4. Thermal radio emissions

The coronal plasma emits thermal radio waves by two physically different mechanisms. It is important to distinguish between these different processes. (*i*) The usually dominant process is the *bremsstrahlung* ('breaking radiation' or free–free emission) of electrons experiencing collisions with other electrons or ions. (*ii*) In active regions, the enhanced magnetic field strength increases the gyration frequency of electrons in the field (Section 2.1.1) and makes *gyroresonance emission* the dominant thermal radiation process between roughly 3 GHz to 15 GHz. This process opens a possibility to measure the coronal magnetic field. High-frequency bremsstrahlung originates usually at high density in the atmosphere. Similarly, the higher the magnetic field, the higher the observed frequency of gyroresonance emission. Therefore, thermal high-frequency sources are generally found at low altitude.

The large range of radio waves is conveniently divided according to wavelength into metric, decimetric, centimetric, etc. radiation (30 – 300 MHz, 0.3 – 3 GHz, 3

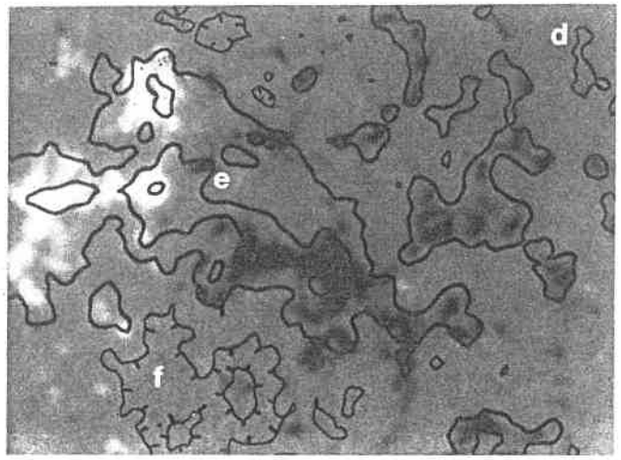

Fig. 1.3. A magnetogram of a decayed (spotless) active region in the left part and quiet photosphere at right is presented as a grayscale image. Positive polarity (where the magnetic field vector points out of the picture) is represented as bright, and negative polarity as dark. Superposed are the contours of the radio intensity at 8.5 GHz observed at the VLA. The size of the total image is 0.36 $R_\odot$. Some particular locations are labelled and discussed in the text (from Gary *et al.*, 1990).

– 30 GHz, etc.). Alternatively, the technical term *microwaves*, meaning the range 1 – 30 GHz, is also frequently used.

Figure 1.3 compares the radiation intensity at 8.5 GHz with the underlying magnetic field strength along the line of sight. The peak brightness temperature of $4.1 \cdot 10^4$ K suggests that radiation originates from the transition region. Model calculations assuming bremsstrahlung emission show that this is the case. Enhanced radio emission correlates with patches of an enhanced photospheric magnetic field (called network) a few 1000 km below, as first noted by M.R. Kundu *et al.* in 1979. The network of the quiet part (*d*) outlines the boundaries of supergranules, formed by large-scale convection cells underneath. The depression in brightness (*f*) coincides with a filament seen in absorption of the Hα line. The magnetic field at the height of the radio source cannot be measured in general, but may be estimated using the photosphere as a boundary surface. The peak radio intensity is above the neutral line of the decayed active region (marked *e* in Fig. 1.3), where the longitudinal field component vanishes and (just below the letter *e*) a weak loop structure seems to bridge the two polarities. The marvellous correlation between magnetic field and transition region suggests that the field also influences the heating of quiet regions.

1.2. Dynamic Processes

1.2.1. Processes in the upper corona

The solar corona is remarkably variable on all time scales. Even the early observers of eclipses noted the different shape of the corona, year after year. The 11-year magnetic cycle, conspicuous in the sunspots of the photosphere, has a striking effect on the corona. During the minimum years the corona shows few streamers, and these have enormous 'helmets' and are located near the equator. In solar maximum years the average density increases, and numerous streamers are more regularly distributed (Fig. 1.1).

Pictures taken by coronagraphs (producing an artificial eclipse) on board spacecraft show more rapid changes. As a rule, structures do not persist long enough to be followed during the few days it takes to traverse the limb. Bright and dark rays appear and disappear within hours. Major events, called *coronal transients*, occur daily during the solar maximum. They are connected (though not always) to coronal mass ejections or flares, and sometimes result in disrupting or dissolving streamers.

1.2.2. Processes in the lower corona

Soft X-ray motion pictures show ceaseless variability in active regions. Loops brighten up and disappear within a few hours. Also, interconnecting loops sometimes light up within hours. Loops that connect an active region to an old remnant remain stable for several days.

Also fascinating are the incessant brightenings in *quiet regions and coronal holes*, as discovered 1997 by S. Krucker *et al.* in soft X-rays and radio emission. They consist of loops, typically 10 000 km long and 2000 km wide, flaring up and fading on time scales of a few minutes. The footpoints of the loops have been found in tiny bipolar regions in photospheric magnetograms. More than a million such microevents can be observed on the whole Sun per hour in the very sensitive coronal EUV lines of Fe IX and Fe XII. Interestingly, the fluctuations do not indicate much heating of already hot plasma, but rather the addition of new plasma presumably of chromospheric origin. The events constitute also an energy input of a sizeable fraction of what is needed to heat the quiet corona.

Duration and size become even smaller in the sources located in the transition region. The radio and UV sources in the quiet regions (Fig. 1.3) vary within less than one hour, sometimes within one minute. Jets of a few thousand kilometers in diameter have been observed in a line of C IV to accelerate upward to speeds as high as 400 km s^{-1} (Brueckner and Bartoe, 1983).

The plasma in active-region loops is in continual motion along the magnetic field lines. Upflows in chromospheric *spicules* and the more dramatic *surges* move typically at a speed of 20 to 30 km s^{-1} and reach heights of 11 000 km and 200 000 km, respectively. *Coronal rain* is a relatively cool plasma observable in the Hα line, flowing down at nearly the free-fall speed of 50 to 100 km s^{-1}.

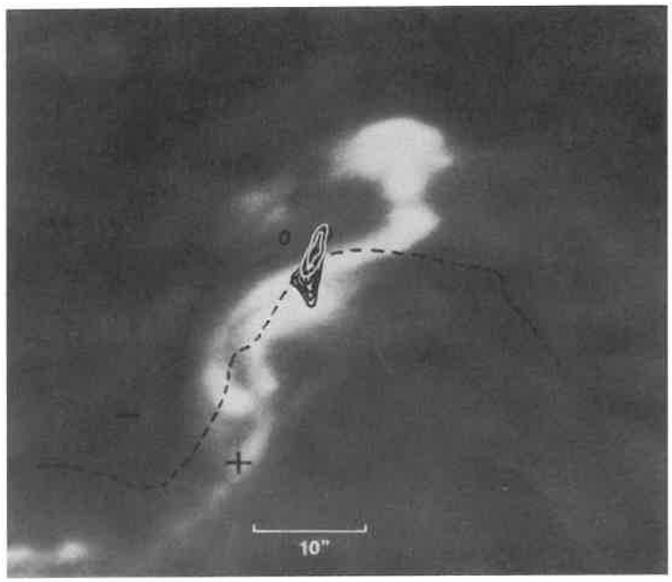

Fig. 1.4. A flare appears bright in a picture taken in the optical Hα line at the Big Bear Observatory. The flare partially follows the line (dashed) of zero longitudinal magnetic field measured in the underlying photosphere. The contours outline the microwave intensity at 15 GHz observed by the Very Large Array. White contours show left circular polarization, black contours show right circular polarization. The scale of 10″ corresponds to 7260 km (from Hoyng *et al.*, 1983).

1.2.3. Solar flares

The *flare* is a process of dramatic and truly remarkable dimensions. Its energy release spans many orders of magnitude, from the smallest microflares observable in EUV lines and radio emission of the solar corona (less than 10^{24} erg) to the most energetic events in young or rapidly rotating late-type stars in stellar clusters (10^{37} erg). The first solar flare was observed as a brightening in white light by R.C. Carrington and R. Hodgson in 1859. The emission originated from a small area in an active region and lasted only a few minutes. When, a few years later, the Sun was studied extensively in the chromospheric Hα line, the reports of flares became much more frequent, but also bewilderingly complex. Variations of source size, ejections of plasma blobs into the solar wind, and blast waves were noted. Meterwave radio emissions, detected serendipitously in 1942 by J.S. Hey during military radar operations, revealed the presence of non-thermal electrons in flares. During a radio burst, the total solar radio luminosity regularly increases by several orders of magnitude.

In the late 1950s it became possible to observe the Sun in hard X-rays by balloons and rockets. L.E. Peterson and J.R. Winckler discovered the first emission during a flare in 1958. Later, the enhancements observed in microwave and hard X-ray emissions have led to the surprising conclusion that these energetic particles contain a sizeable fraction (up to 50%) of the initial flare energy release. The broadband microwave emission results from the gyration of mildly relativistic electrons in the magnetic field (gyrosynchrotron emission, Section 8.1.2). Hard X-rays ($\geq$ 10 keV) are caused by electrons of similar energies having collisions (Section 6.4). In 1972 the γ-ray emission of heavy nuclei excited by MeV protons was discovered. This emission indicates accelerated ions (Section 7.1.1). Finally, EUV and soft X-ray ($<$ 10 keV) emissions have shown that the flare energy heats the plasma of coronal loops to temperatures from 1 to $3 \cdot 10^7$ K. Within minutes, some active-region loops become brilliant soft X-ray emitters, outshining the rest of the corona. Obviously, such temperatures suggest that the flare is basically a coronal phenomenon.

One may thus define the flare observationally as a brightening within minutes of any emission across the electromagnetic spectrum. The different manifestations seem to be secondary responses to the same original process, converting magnetic energy into particle energy, heat, and motion.

The timing of the different emissions of the same flare is presented schematically in Fig. 1.5. In the *preflare phase* the coronal plasma in the flare region slowly heats up and is visible in soft X-rays and EUV. The large number of energetic particles is accelerated in the *impulsive phase*, when most of the energy is released. Some particles are trapped and produce the extended emissions in the three radio bands. The thermal soft X-ray emission usually reaches its maximum after the impulsive phase. The heat is further distributed during the *flash phase*. In the *decay phase*, the coronal plasma returns nearly to its original state, except in the high corona ($\gtrsim 1.2\ R_\odot$), where plasma ejections or shock waves continue to accelerate particles causing meter wave radio bursts and interplanetary particle events (Section 10.2).

1.2.4. Other dynamic processes

Somehow related to flares in their physics, but even more powerful, are *coronal mass ejections (CME)* which will be discussed in Section 10.2.3. The first observers of CMEs in optical lines (using ground-based coronameters) describe the events as 'coronal depletions' (e.g. Hansen *et al.*, 1971). The full scope of CMEs was not realized until 1973, when white-light observations were possible from space by the Skylab mission. CMEs occur when a coronal structure – a system of loops or a prominence – loses its equilibrium and starts to rise. Such events carry away remarkable amounts of coronal mass (up to 10^{16} g) and magnetic flux; most of their energy does not show up in the brightening of some radiation or flare. CMEs reach velocities of several hundred km s^{-1} and can be followed on their path throughout the heliosphere.

Radio *noise storms* are also relatives of flares (Section 9.5.2). They were identified soon after the discovery of the solar radio emission. Noise storms consist

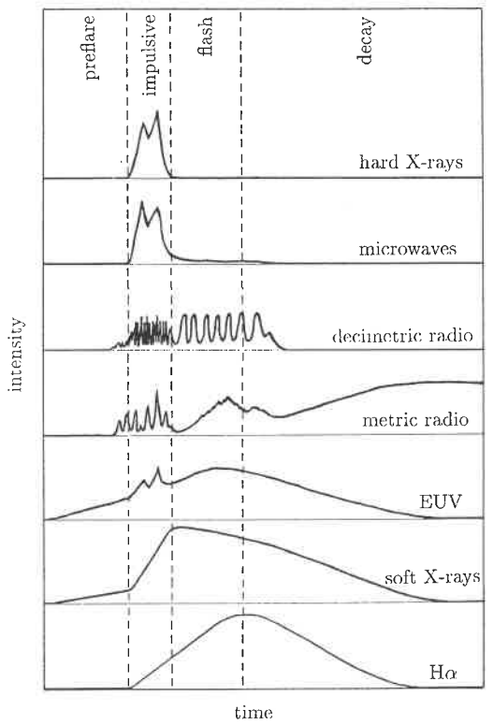

Fig. 1.5. A schematic profile of the flare intensity at several wavelengths. The various phases indicated at the top vary greatly in duration. In a large event, the preflare phase typically lasts ten minutes, the impulsive phase one minute, the flash phase five minutes, and the decay one hour.

of myriads of tiny meter wave bursts of duration about a second or less, and a broadband, slowly varying continuum ranging from 60 to 400 MHz. The storms last for days and are not directly associated to flares, although the start of noise storms may be initiated by a large flare or a CME. More frequently, storms appear in the upper corona (> 1.2 $R_\odot$) when a new active region forms or rapidly grows. This suggests that they represent the adjustment of the previous coronal plasma and magnetic field to the newly emerged magnetic flux.

The various dynamic processes discussed in this section represent energy inputs in different forms. Are they enough to heat the solar corona? The answer seems to become more difficult the more we know about the corona. Regular flares in active regions release most energy by the largest events. They are not frequent enough to account for the quasi-steady heating of the entire corona. Microflares similar to noise storm sources but at low height having energies below 10^{26} erg may provide the energy in active regions. It has been proposed that microevents and network sources heat the quiet corona and coronal holes. Note that additional forms of

energy input, in particular by waves and stationary electric currents, must also be considered. The heating problem of the solar corona can only be solved by a better understanding of all the various processes.

1.3. Stellar Coronae

1.3.1. Soft X-ray emission

The Sun was the only star known to possess a high temperature corona until X-ray telescopes became feasible. There was no great hope of detecting other coronae with the first soft X-ray instruments. Capella, a nearby binary system of two late-type giants, was discovered in 1975 when the X-ray detector of a rocket payload was briefly pointed at the object (Catura *et al.*, 1975), a detection soon confirmed by satellite (Mewe *et al.*, 1975). Capella's corona was found to be a thousand times more luminous than the Sun!

The discoveries of other coronae, and in particular of coronae of other types of stars, followed slowly until the launch of the Einstein satellite. Its greatly superior sensitivity revealed that particular stars of nearly all types are X-ray emitters (Vaiana *et al.*, 1981). Figure 1.6 gives an overview of different types of prominent X-ray stars. Note that X-ray emissions from stars earlier than type A have a different origin. The strong X-ray emission of O and B stars is caused by hot stellar winds. Late-type (F to M) stars on the main sequence have coronae similar to the Sun with a wide range of luminosities for each spectral type. The dependence on photospheric temperature and – even more surprisingly – on photospheric radius is small.

The post-T Tau stars indicated in Figure 1.6 are of particular interest. They are a class of young stars that have evolved beyond the accretion phase (being so-called weak-line T Tau stars), but have not yet arrived on the main sequence. BY Dra and RS CVn stars are binary systems with no significant mass exchange, but close enough so that the tidal effects of their gravitational interaction synchronize the rotation periods of the individual stars to the orbital period of the system. Since the orbital periods range from less than a day to a few days, the stars are forced to rotate rapidly. In BY Dra systems both components are late-type, main-sequence stars; in RS CVn systems at least one component is a subgiant. FK Com stars are even more rapidly rotating objects and may be the remnants of collapsed binary systems.

The X-ray luminosity given in Figure 1.6 indicates a minimum requirement on the coronal heating process. The actual energy input is higher if there are energy losses other than radiation. Since we do not yet have good stellar models, the Sun may serve as an example. Conduction losses of the solar corona to the underlying chromosphere have been estimated as 50% in quiet regions, but less in active regions. In coronal holes, about 90% of the input energy ends in solar wind expansion (Withbroe and Noyes, 1977).

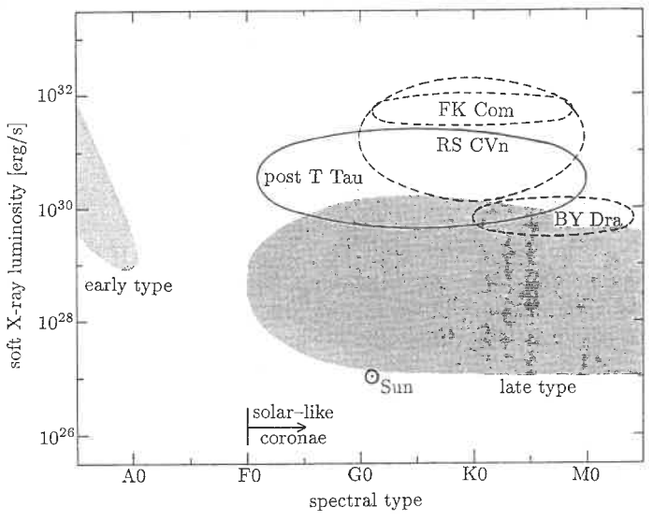

Fig. 1.6. Thermal soft X-ray emission of hot stellar plasma has been observed from nearly all types of stars. The spectral type characterizes the temperature of the photosphere and is also an indication of stellar mass (decreasing to the right). X-ray emitting main-sequence stars are represented by shading, young main-sequence stars (post T Tauri type) by full contours, and binary systems of BY Draconis and RS Canem Venaticorum types, as well as 'post-binaries' of FK Draconis type, by dashed curves.

The range of solar-like coronae overlaps approximately with the stellar types that have a convection zone below the photosphere. Another necessary condition is stellar rotation: the faster a star rotates, the more luminous the corona (Pallavicini *et al.*, 1981).

In open field regions the hot coronal plasma expands thermally and forms a stellar wind. The loss of angular momentum carried away by the wind is the likely cause of the present day slow equatorial rotation of the Sun in 26 days, compared to ten times faster rates in young main-sequence stars. Observing star clusters of different age, O. Struve and others found in 1950 that a braking process operates for young main-sequence stars of type F and later. The existence of coronae seems to be important in slowing down the rotation of late-type stars.

1.3.2. Stellar flares

The existence of stellar coronae could have been guessed from stellar flares, known for half a century. As in the case of the Sun, stellar flares were first detected in white light. In K and M main-sequence stars having low intrinsic optical luminosity, the effect of a flare on the layers below is more easily observable than in the Sun. Flares temporarily increase the total stellar luminosity. In UV light (U-band) this may reach a factor of ten.

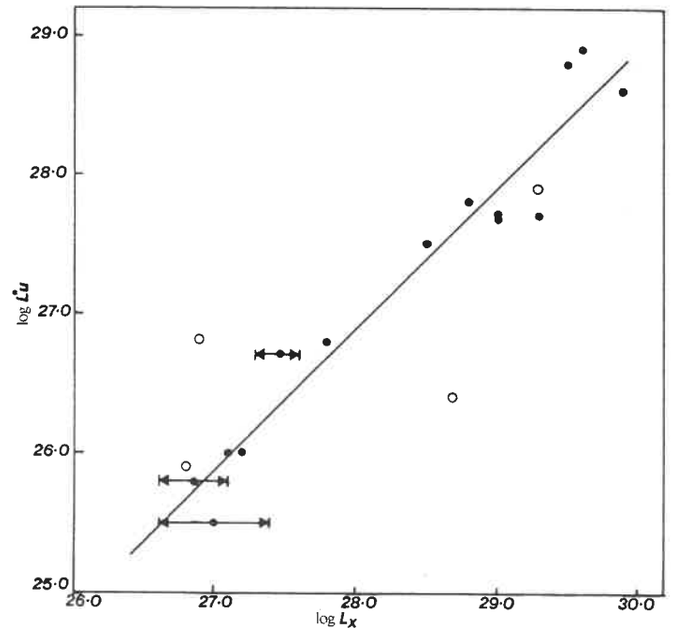

Fig. 1.7. The time averaged luminosity of flare emission in the ultraviolet, L_u^*, is compared to the quiescent soft X-ray emission, L_x, for nearby main-sequence M stars (from Doyle and Butler, 1985).

Stellar flares have also been detected in radio, EUV, and soft X-ray emissions (Section 8.4.4). Reliable and frequent measurements became possible around 1980 with the Very Large Array (a radio interferometer in New Mexico) and the Einstein satellite, respectively. The radio flares exist as at least two types: short ($\lesssim$ 10 minutes), circularly polarized events not associated with optical or X-ray emissions; and long-duration, weakly polarized events ($\lesssim$ 40%) coincident with optical and X-ray flares.

Flaring has been reported in all spectral classes along the main sequence, both on single stars and on members of multiple systems. Flare activity starts at an early phase of stellar evolution, and flaring is particularly frequent in pre-main-sequence stars. Most importantly, stars with considerable coronae are likely to have frequent flares. The integrated luminosity in X-rays of one flare ranges from the detection limit of 10^{27} erg in nearby M stars to 10^{37} erg in star clusters.

Figure 1.7 shows an important discovery, made independently in 1985 by J.G. Doyle and C.J. Butler, D.R. Whitehouse, and A. Skumanich. They found a tight correlation between the time averaged luminosity of U-band flares and the quiescent X-ray luminosity in dMe, a subclass of main-sequence (*dwarf*) M stars with chromospheric emission (*e*) lines. A relationship between quiescent and flaring activity is not unexpected from the solar observations. They show that (*i*) the

heating of coronal regions is connected to the magnetic field and that (*ii*) the flare energy is drawn from the same magnetic field. Thus both originate from the same dynamo process in the stellar interior that generates the magnetic field.

1.3.3. Quiescent radio emission

The discovery of a low-level microwave emission ($\gtrsim 1$ GHz) from apparently non-flaring, single dMe stars in 1981 by D.E. Gary and J.L. Linsky has added another mystery to coronal physics. The radiation is 2–3 orders of magnitude more luminous than the quiet Sun. Spectral investigations and VLBI measurements of the source size have shown that the radio emission must originate from more energetic electrons than the X-rays. It is probably non-thermal. In contrast, the quiet and slowly varying solar radio emissions are caused thermally and by the same plasma that emits soft X-rays. The different word 'quiescent' has been chosen for stars to indicate the difference from the solar non-flare radio emissions and to emphasize the possibility that the observed low-level variability (on time scales longer than ten minutes) may, in fact be a superposition of many flare-like events. The typical quiescent stellar radiations have a brightness temperature of some 10^9 K and are often weakly polarized. This is compatible with an interpretation by gyrosynchrotron emission of a population of energetic ($\gtrsim 100$ keV) electrons spiraling in the coronal magnetic field. The presence of such particles is ubiquitous during solar flares (Section 1.2.3), but does not noticeably contribute to the quiet solar radio emission. The gyrosynchrotron emission, however, permanently dominates the microwave emission of dMe stars, surpassing the thermal solar radio luminosity by orders of magnitude.

Figure 1.8 is the gist of a decade of painstaking measurements by many observers and instruments. The quiescent soft X-ray and microwave emissions are compared not only for different stars and types of stars, but also with the temporary sources of solar flares. The correlation between thermal emission and radiation of non-thermal particles is obvious and stretches over many orders of magnitude. It tells us that the continuous presence of accelerated particles and coronal heating have something in common. Figure 1.8 supports the conjecture that a common process in the stellar interior drives the coronal heating and flares. Moreover, the similarity of flares and coronae suggests a more direct relation between the thermal constituent of coronal plasmas and powerful, possibly violent acceleration processes in the corona. The heating of the coronae of rapidly rotating stars and flares both accelerate electrons and may be similar processes!

Are coronal plasmas heated by flares? The answer is not simple, as it has become clear in Section 1.2 that there are different types of flare-like, dynamic processes even in a relatively inactive corona like the Sun's. There is substantial variability in the X-ray and radio emissions of most stellar coronae over a variety of time scales. The observed variability is in the form of individual flares and slow variations of the quiescent background. Flares show a wide range of amplitude (up to a factor of 10), whereas the variations of the quiescent component on time scales of hours do not exceed amplitudes of 50%. Continuous low-amplitude, short-period

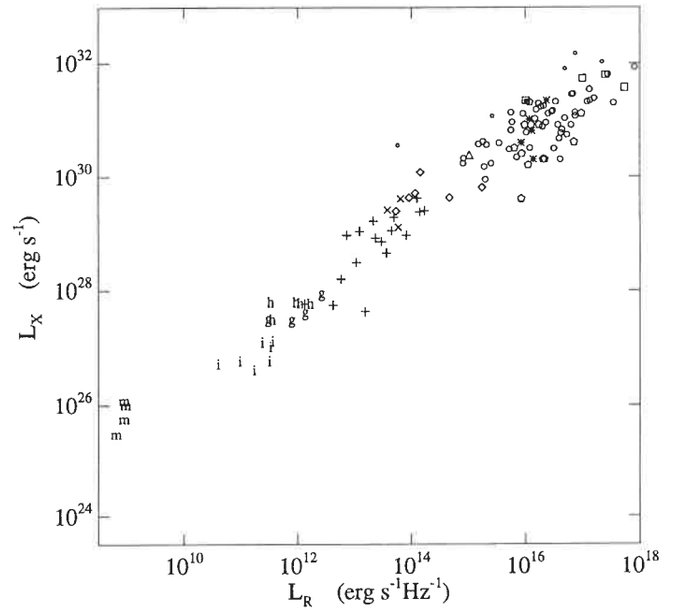

Fig. 1.8. The soft X-ray luminosity is plotted vs. the radio luminosity at a frequency of 5–10 GHz. Different types of stars are compared with the peak flux of solar flares. Key to the symbols: *m* solar microflare; *i* intermediate impulsive solar flare; *h* gradual solar flare with dominating large impulsive phase; *g* pure gradual solar flare; + dM(e) stars; × dK(e) stars; ◇ BY Dra binaries; ◯ RS CVn binaries; ○ RS CVn binaries with two giants; △ AB Dor; ∗ Algols; □ FK Com stars; (pentagon) post-T Tau stars (from Benz and Güdel, 1993).

variability (microflares) has been proposed for the heating of stellar coronae, but the observational evidence is still meager.

In conclusion, observations – both solar and stellar – strongly suggest that it is not possible to comprehend coronae without understanding their dynamic phenomena. Apart from the heating problem, coronal processes offer numerous and exciting challenges for plasma astrophysics in general. Some of them will be introduced as applications throughout the book.

1.4. Fundamental Equations

When a gas like a corona is heated beyond its atomic binding energy, collisions strip off electrons from the atoms. Freely moving electrons and ions eventually recombine, but may become ionized again. The two rates cancel in equilibrium. This fourth state of matter behaves peculiarly in the presence of electric and magnetic fields. We shall call an ionized gas a *plasma*, if the free charges are abundant

enough to influence the relevant properties of the medium. The equilibrium fraction of neutral atoms is given by the Saha-Boltzmann ionization equation. As an example, the ratio of neutral to ionized atoms is $5 \cdot 10^{-17}$ for a hydrogen plasma with a density of 10^8 cm^{-3} at a temperature of 10^6 K. These values are typical of the solar and some stellar coronae. We shall neglect the influence of the neutrals in the following, and thus consider only fully ionized plasmas.

Let us consider the motion of a particle i with charge q_i, mass m_i, velocity $\mathbf{v}_i$, and Lorentz-factor γ_i. In electrodynamics the particle is influenced by the Coulomb force due to the electric field $\mathbf{E}$ and the Lorentz force due to the magnetic field $\mathbf{B}$ (sometimes also called magnetic flux density or magnetic induction). The equation of particle motion is Newton's second law, which equates the temporal derivative of the momentum with the forces acting on the particle. This basic equation provides a first connection between particles and fields,

$$\frac{\partial}{\partial t}(m_i \gamma_i \mathbf{v}_i) = q_i(\mathbf{E} + \frac{1}{c}\mathbf{v_i} \times \mathbf{B}) \quad . \tag{1.4.1}$$

We are using Gaussian (cgs) units. A conversion table to mks units can be found in Appendix B. Vector variables are signified by bold face or underbars. Tensor variables are, in the following, indicated by hats. The product of two vectors is defined in Appendix A in three ways: scalar product (indicated by $\cdot$), vector product (indicated by $\times$), and tensor product (indicated by $\circ$). We consider the particles of a plasma to move in a vacuum, and therefore the dielectric tensor equals the unity tensor ($\hat{\epsilon} = \hat{1}$), and similarly the magnetic permeability $\hat{\mu} = \hat{1}$. The electromagnetic fields are given by Maxwell's equations, which then reduce to:

$$\nabla \times \mathbf{B} = \frac{4\pi}{c}\mathbf{J} + \frac{1}{c}\frac{\partial \mathbf{E}}{\partial t} \tag{1.4.2}$$

$$\nabla \times \mathbf{E} = -\frac{1}{c}\frac{\partial \mathbf{B}}{\partial t} \tag{1.4.3}$$

$$\nabla \cdot \mathbf{B} = 0 \tag{1.4.4}$$

$$\nabla \cdot \mathbf{E} = 4\pi\rho^* \quad . \tag{1.4.5}$$

∇ is the operator $(\partial/\partial x, \partial/\partial y, \partial/\partial z)$, which can be treated like a vector. We shall refer to it as the *nabla* operator, after the Phoenician stringed instrument having the same shape. ∇^2 is the scalar product of two such operators, $\partial^2/\partial^2 x + \partial^2/\partial^2 y + \partial^2/\partial^2 z$; it is generally termed the Laplace operator. $\nabla\times$ is the *curl* (or rotation), and $\nabla\cdot$ is the divergence (cf. definitions A.4 and A.5 in Appendix A). The electric charge density ρ^* and the current density $\mathbf{J}$ are defined by the sums over all particles i in an elementary volume $\Delta\mathcal{V}$,

$$\rho^* := \frac{1}{\Delta\mathcal{V}} \sum_{i,\Delta\mathcal{V}} q_i \quad , \tag{1.4.6}$$

$$\mathbf{J} := \frac{1}{\Delta\mathcal{V}} \sum_{i,\Delta\mathcal{V}} q_i \mathbf{v}_i \quad , \tag{1.4.7}$$

providing a second link between particles and fields.

Equation (1.4.2) is Ampère's law complemented by the displacement current. It states that either electric currents or time-varying electric fields may produce magnetic fields and *vice versa*. Equation (1.4.3) is credited to Faraday and Equation (1.4.5) to Poisson, implying the origin of electric fields by time-varying magnetic fields and electric charges, respectively. Equation (1.4.4) expresses the absence of magnetic monopoles.

Since each particle obeys Equation (1.4.1), the system of Equations 1.4.1) – (1.4.7) is complete. It can, in principle, be solved if the particle masses, charges, initial positions, and velocities are known. The charged particle motions create the electromagnetic fields, which in turn influence the motion of the particles. A coupled system of this kind is obviously highly non-linear.

The large number of equations of the kind of (1.4.1) inhibits the solution of the system (1.4.1) – (1.4.7) for real cosmic plasmas, even using the fastest computer available. One has the choice of reducing the particles to a tractable number, or of using appropriate statistical methods. Numerical simulations generally overcome the non-linearities. Analytical and statistical calculations render a better overview and understanding of the physics.

1.4.1. MAGNETOHYDRODYNAMIC APPROACH

There are two major statistical approaches to plasma physics. One, generally termed *magnetohydrodynamics (MHD)*, assumes that the plasma can be sufficiently described by a fluid, i.e. by velocity averaged parameters such as density n, mean velocity $\mathbf{V}$, temperature T, etc.,where

$$n := \int f(\mathbf{v}) d^3v \quad , \tag{1.4.8}$$

$$\mathbf{V} := \frac{1}{n}\int \mathbf{v} f(\mathbf{v}) d^3v \quad , \tag{1.4.9}$$

$$T := \frac{m}{3k_B n}\int (\mathbf{v} - \mathbf{V})^2 f(\mathbf{v}) d^3v \, , \tag{1.4.10}$$

and $f(\mathbf{v})$ is the velocity distribution given by the mean number of particles per volume element in space and velocity. Equation (1.4.8) can be considered as the normalization of f. In Equations (1.4.8) – (1.4.10) we have simplified to the non-relativistic case. Conservation of particle number, total momentum and energy, combined with Maxwell's equations and an equation of state – after some simplifying approximations – form a complete system of a more humanly manageable number of equations (to be discussed in Chapter 3.1).

Gradual plasma processes in coronae do not require a description at the detail of the particle level. MHD is widely used to study equilibrium conditions and

the onset of global instabilities. Ideal MHD does not include electric fields parallel to the magnetic field, and neglects populations of energetic particles cospatial with the thermal background of rapidly colliding particles. We shall find MHD extremely useful if the velocity distributions are close to Maxwellian. This is certainly the case in thermal equilibrium and small deviations from it. Collisions (and other randomizing processes) tend to bring any distribution toward a Maxwellian shape, the maximum entropy distribution.

MHD becomes questionable for processes which are faster than the collision time. Such a period may seem too short to be relevant. However, in certain plasma phenomena *collisionless* processes (occurring much faster than the time between collisions) have turned out to control the situation. Let us illustrate by three examples how this can happen. (*i*) High-frequency waves can grow within a fraction of the collision time, absorb a considerable fraction of the total energy, and change drastically the plasma resistivity. (*ii*) Electric fields, both stationary or in waves, can rapidly accelerate charged particles so that their velocity distribution deviates considerably from a Maxwellian form. (*iii*) The collision time of energetic particles increases with the third power of velocity (Section 2.6). High energy particles thus have long collision times. They may spread over a large volume and form a population of particles that can be considered 'collisionless' over time scales of minutes to hours.

1.4.2. KINETIC APPROACH

The other statistical approach, *kinetic plasma physics*, starts at a much lower level, considering particle orbits and the properties of $f(\mathbf{v})$ without integration in velocity. The basic equation, named after L. Boltzmann, will be derived from particle conservation in Chapter 3,

$$\frac{\partial f}{\partial t} + \mathbf{v}\frac{\partial f}{\partial \mathbf{x}} + \frac{q}{m}(\mathbf{E} + \frac{1}{c}\mathbf{v} \times \mathbf{B})\frac{\partial f}{\partial \mathbf{v}} = \left(\frac{\partial f}{\partial t}\right)_{\text{coll}} . \qquad (1.4.11)$$

The electromagnetic fields have been split into macroscopic components and microscopic components. The macroscopic part is denoted $\mathbf{E}$ and $\mathbf{B}$, the spatial averages over a volume much larger than the Debye shielding length (Chapter 2.4). The rapidly fluctuating fields of the neighboring particles are taken care of by the *collision term* on the right hand side. We do not need to apply quantum mechanics as long as the interparticle distance exceeds the de Broglie wavelength of the particles (but note quantum effects in close collisions, Eq. 2.6.17) and the photon energies are smaller than the rest mass of the particles. For a more complete introduction and discussion of this fundamental equation the reader is referred to Section 3.1.1.

The full scope of kinetic plasma physics of the universe cannot be estimated yet. In the realm of stars, it is mainly the hot, dilute coronae where collisionless plasma processes occur. As an example, let us look at the collision time of thermal electrons as a function of height in the solar atmosphere (Figure 1.9). It increases more than six orders of magnitude from the bottom of the chromosphere to the

corona. In the chromosphere, collisions of a charged test particle are mostly with neutral atoms. The collision time increases with height as the material becomes less dense, but decreases again as the temperature (and mean velocity of the electrons) increases. It has a narrow minimum at the bottom of the transition region where the dominant collision partners change from neutrals to charged particles, and it becomes orders of magnitude larger in the hot corona.

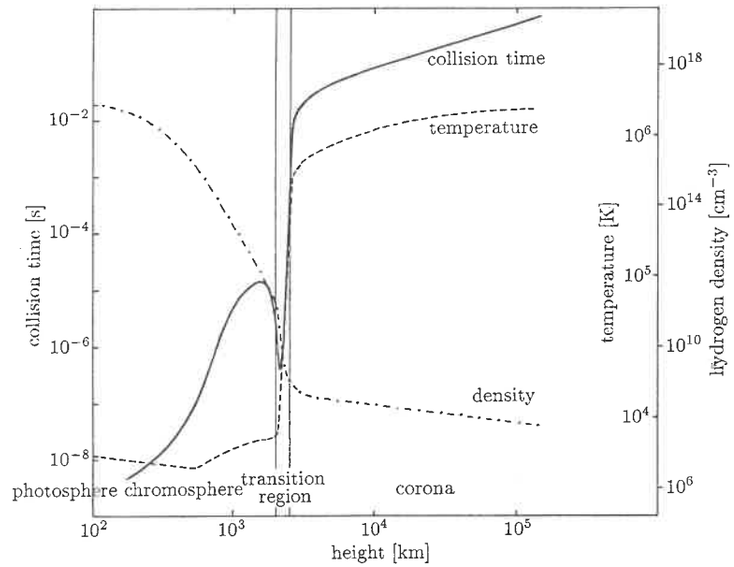

Fig. 1.9. Schematic drawing of the collision time vs. height of an electron moving at the mean thermal velocity in the quiet solar atmosphere. The relevant plasma parameters are from standard models and are also shown (dashed). The hydrogen density includes both neutral atoms and ions.

Other fields for applying kinetic plasma physics include magnetospheres of planets and neutron stars, extended atmospheres of stars in formation, accretion discs, supernova remnants, and cosmic rays. Even some massive (early-type) stars show signs of energetic particles and magnetic activity.

Plasma physics at the particle level may be required in very localized regions during times of rapid change. Such processes, however, may be at the heart of some of the classical, unsolved coronal phenomena. Let us consider ten key examples of kinetic plasma processes in coronae:

- High energy particles are widely observed in the universe; *particle acceleration* has various origins. The most basic mechanism is simply a quasi-static electric

field. In turn, accelerated particles drive collisionless plasma waves to grow unstably and may alter the acceleration process (Section 4.6).

- Interactions of plasma waves with particles in resonance cause various phenomena where energy is exchanged between waves and particles (Chapter 5). The result is either *heating* (more general: energization) of certain particle species or unstable growth of some other wave modes.
- Wave-particle interactions cause *anomalous (i.e. additional) resistivity* in an electric current. It can rapidly release the free energy of a strong current or, in other words, of its associated magnetic field (Chapter 9).
- Wave-particle interactions also increase viscosity and generally change the *transport coefficients* of a plasma. They have the effect of additional collisions.
- *Collisionless shock waves* can also accelerate particles and heat. They are sites of enhanced turbulence of various wave modes (Chapter 10).
- *Particle beams* are frequently observed in the solar corona and in interplanetary space cospatial with the background plasma. Beams can be signatures of some cosmic accelerator, or can form simply by evaporation from an impulsively heated source (Section 2.3).
- Beams are often unstable to *growing plasma waves* in the background plasma. The wave turbulence thrives on the beam energy and accompanies the beam until exhaustion (Chapters 6 and 7).
- Energetic particles having long collision time can be *trapped in magnetic mirror* configurations that are abundant in the form of coronal loops or dipole fields. A large number of fast particles accumulate near the acceleration region (Chapter 8). The velocity distribution of magnetically trapped particles, having the form of a *loss-cone*, gives rise to several instabilities of growing collisionless waves. They may control the trapping time (Section 8.3).
- Some kinetic processes cause *observable electromagnetic radiation*. Plasma wave turbulence of various origins can emit electromagnetic radiation by wave-wave coupling (Section 6.3). Such emissions yield information on plasma processes in cosmic sources. Another example is one of the loss-cone instabilities driving electromagnetic waves. This very efficient emission corresponds to a *maser* process, whereby electrons change gyration orbits (Section 8.2).
- Large amplitude waves develop *non-linear structures*, such as solitons. Their energy density is a considerable fraction of the thermal background. Furthermore, they can be powerful emitters of coherent radiation.

One sometimes notes in plasma astrophysics, and particularly in coronal physics, a gap between observation and theory. This disparity, which hinders progress in the field, exists for several reasons. (*i*) Plasma phenomena – in particular kinetic processes – tend to have many parameters, and they are often not observable. Therefore, theories are difficult to test by observations. (*ii*) Scientists in the field separate into observers and theoreticians early in their career and so lose the capability to combine the two tools. This book intends to bridge this gap.

Further Reading and References

Introductory texts into solar physics

Bray, R.J., Cram, L.E., Durrant, C.J., and Loughead, R.E.: 1991, *Plasma Loops in the Solar Corona*, Cambridge Astrophysics Series, Vol. **18**, Cambridge University Press.

Durrant, C.J.: 1988, *The Atmosphere of the Sun*, Hilger, Bristol UK.

Stix, M.: 1989, *The Sun*, Springer, Berlin.

Tandberg-Hanssen, E. and Emslie, A.G.: 1988, *The Physics of Solar Flares*, Cambridge University Press, Cambridge UK.

Zirin, H.: 1987, *Astrophysics of the Sun*, Cambridge University Press, Cambridge UK.

Reviews and articles on stellar coronae

Güdel, M.: 1994, 'Non-Flaring Stellar Radio Emissions', *Astrophys. J. Suppl.* **90**, 743.

Linsky, J.L.: 1985, 'Non-radiative Activity Across the HR-diagram: Which Types of Stars are Solar-like?', *Solar Phys.* **100**, 333.

Greiner, J., Duerbeck, H.W., and Gershberg, R.E. (eds.): 1995, 'Flares and Flashes', IAU Coll. 151, *Lecture Notes in Physics* **454**.

Haisch, B., Strong, K.T., and Rodonó, M.: 1991, 'Flares on the Sun and Other Stars', *Annual Rev. Astron. Astrophys.* **29**, 275.

Narain, U. and Ulmschneider, P.: 1991, 'Chromospheric and Coronal Heating Mechanisms', *Space Sci. Rev.* **57**, 199.

Schmitt, J.H.M.M.: 1990, 'X-ray Astronomy', *Adv. Space Res.* **10**, 115.

References

Benz, A.O. and Güdel, M.: 1993, 'Radio and X-Ray Observations of Flares and Coronae', *Astron. Astrophys.* **285**, 621.

Benz, A.O. and Krucker, S.: 2002, 'Energy Distribution of Micro-events in the Quiet Solar Corona', *Astrophys. J.*, in press.

Brueckner, G. and Bartoe, J.: 1983, 'Observations of High-Energy Jets in the Corona above the Quiet Sun, the Heating of the Corona, and the Acceleration of the Solar Wind', *Astrophys. J.* **272**, 329.

Catura, R.C., Acton, L.W., and Johnson, H.M.: 1975, 'Evidence for X-Ray Emission from Capella', *Astrophys. J.* **196**, L47.

Doyle, J.G. and Butler, C.J.: 1985, 'Ultraviolet Radiation from Stellar Flares and the Coronal X-Ray Emission for Dwarf-M_e Stars', *Nature* **313**, 378.

Gary, D.E., Zirin, H., and Wang, H.: 1990, 'Microwave Structure of the Quiet Sun at 8.5 GHz', *Astrophys. J.* **355**, 321.

Hansen, R.T., Garia, C.J., Grognard, R.J.-M., Sheridan, K.V.: 1971, 'A Coronal Disturbance Observed Simultaneously with a White-Light Coronameter and the 80 MHz Culgoora Radioheliograph', *Proc. Astron. Soc. Australia* **2**, 57.

Hoyng, P., Marsh, K.A., Zirin, H., and Dennis, B.R.: 1983, 'Microwave and Hard X-Ray Imaging of a Solar Flare on 1980 November 5', *Astrophys. J.* **268**, 879.

Krucker, S., Benz, A.O., Acton, L.W., and Bastian, T.S.: 1997, 'X-ray Network Flares of the Quiet Sun', *Astrophys. J.* **488**, 499.

Kundu, M.R., Rao, A.P., Erskine, F.T., and Bregman, J.D.: 1979, 'High Resolution Observations of the Quiet Sun at 6 Centimeters Using the Westerbork Synthesis Radio Telescope', *Astrophys. J.* **234**, 1122.

Mewe, R. *et al.*: 1975, 'Detection of X-Ray Emission from Stellar Coronae with ANS' *Astrophys. J.* **202**, L67.

Pallavicini, R., Golub, L. Rosner, R., Vaiana, G.S. Ayres, T., and Linsky, J.L.: 1981, 'Relation between Rotation and Luminosity', *Astrophys. J.* **248**, 279.

Vaiana, G.S. *et al.*:1981, 'Results from an Extensive Einstein Stellar Survey', *Astrophys. J.* **245**, 163.

Withbroe, G.L. and Noyes, R.W.: 1977, 'Mass and Energy Flow in the Solar Chromosphere and Corona', *Ann. Rev. Astron. Astrophys.* **15**, 363.